



## INTERNATIONAL JOURNAL OF ENGINEERING SCIENCES & RESEARCH TECHNOLOGY

### Numerical Appraisal of Heat Transfer and Flow in Concentric Annuli Permeable and Impermeable Fins by using Nanofluids

**Dr. Khalid Faisal Sultan**

Lecture, Electromechanical. Eng. Dept, University of Technology

#### Abstract

Numerical study was carried out to investigate the natural convection heat transfer enhancement by using utilizing various nanofluids in a three – dimensional annulus. The annulus between two concentric cylinders with porous (permeable) fins, solid (impermeable) fins, without fins and these fins attached to the inner cylinder. The inner cylinder and two fins are maintained at constant wall temperature (CWT), while the outer cylinder is diathermal (adiabatic). The problem was solved numerically using Alternating Direction Implicit (ADI) method. The two types of nanoparticles used in his article metallic silver copper (Cu) and nonmetallic zirconium oxide (ZrO<sub>2</sub>). The numerical results for three cases considered are given in terms of stream function contours and isotherms for values of Rayleigh number Ra of 10<sup>3</sup>, 10<sup>4</sup> and 10<sup>5</sup> and volume fractions  $\Phi$  of 1%, 2% and 5%. As well as this article indicating to the effect fin inclination angles and annulus inclination angles. The numerical results show that As the solid volume fraction increases, the heat transfer is enhanced for all values of the Rayleigh number and volume fraction. Nanoparticles concentration did not reveal serious effect on the secondary flow and the average skin friction coefficient while increasing volume fraction and Rayleigh number significantly increase Nusselt number. The values of the average Nusselt number by using nanofluids are compared with distilled water for three cases porous fins, solid (impermeable) fins, without fins. Results showed that the annulus porous fins provided higher heat transfer rate than annulus solid (impermeable) fins and annulus without fins. The enhancement in heat transfer of nanofluids for annulus with porous fins, solid (impermeable) fins and annulus without fins at (5 %) volume concentration of (Cu) nanoparticles increases (82.25 %, 70.15 %, 50.33 %), while of (ZrO<sub>2</sub>) (69.35 %, 52.44 %, 37.42 %) respectively compared with the base fluid (distilled water).

**Keywords:** Nanofluid, porous fins, solid fins, Heat transfer enhancement.

#### Introduction

Heat transfer within horizontal annuli has many engineering applications especially in heat exchangers, solar collectors, thermal storage systems, and electronic components. Several applications use natural convection as the main heat transfer mechanism. Therefore, it is worth to understand the thermal behavior of such systems when natural convection is important. The first extensive research on this flow geometry was done by Kuhen and Goldstein [1, 2]. In their work, an experimental and numerical investigation was done when the ratio of gap width to inner cylinder diameter was 0.8 for water and air in the annulus. In their experimental study, it was found that transition from laminar to turbulent flow occurs at Rayleigh number of 10<sup>6</sup>. Kumar [3] studied natural convection in horizontal annuli, where the inner cylinder is heated by the application of a constant heat flux and the outer cylinder is isothermally cooled. Ho et al. [4] investigated the natural convection in concentric and eccentric horizontal cylindrical annuli with mixed boundary conditions using numerical methods. They realized that the heat transfer and fluid flow are dependent on the Rayleigh number and eccentricity of the annulus. A numerical investigation for three dimensional natural convection inside horizontal concentric annulus with specified wall temperature and heat flux was done by Chun lang Yeh [5]. An essential restriction in natural convection in an annulus is that the heat transfer rate is limited. Using radial fins on the outer surface of inner cylinder has significant effect on heat transfer rate in the annulus. Having such fins, improves the flow and heat transfer characteristics. Chai and Patankar [6] investigated natural convection heat transfer in an annulus having six radial fins attached to the inner cylinder arranged in two different configurations. It was observed that orientation of the internal fins has no important effect on the average Nusselt number, even though the blockage due to the fins has significant effect on the flow and temperature fields.

Turbulent natural convection between two horizontal concentric cylinders in the presence of radial fins was studied numerically by Rahnema and Farhadi [7]. They observed that higher fins have a blocking effect on flow and cause a lower heat transfer rate, so that there is a reduction in heat transfer rate compared to the case of no fin, at the same Rayleigh number. Nowadays, enhancement of heat transfer attracts the researchers' attention. The low thermal conductivity of conventional heat transfer fluids, such as water, is considered a primary limitation in enhancing the heat transfer performance. Maxwell's study [8] showed the possibility of increasing the thermal conductivity of a fluid–solid mixture by increasing the volume fraction of solid particles. Thus, the particles with micrometer or even millimeter dimensions were used. Those particles caused several problems such as abrasion, clogging, and pressure losses. During the past decade the technology of producing particles in nanometer dimensions was improved and a new kind of solid–liquid mixture that is called nanofluid, was established [9]. The dispersion of a small amount of solid nanoparticles in conventional fluids such as water or Ethylene glycol changes their thermal conductivity remarkably. In general, in most recent research areas, heat transfer enhancement in forced convection is desirable [10–12], but there is still a debate on the effect of nanoparticles on heat transfer enhancement in natural convection applications. Natural convection of  $\text{Al}_2\text{O}_3$  – water and  $\text{CuO}$  – water nanofluids inside a cylindrical enclosure heated from one side and cooled from the other side was studied by Putra et al. [13]. They found that the natural convection heat transfer coefficient was lower than that of pure water. Wen and Ding [14] investigated the natural convection of  $\text{TiO}_2$  – water in a vessel composed of two discs. Their results showed that the natural convection heat transfer coefficient decreases by increasing the volume fraction of nanoparticles.

Jou and Tzeng [15] conducted a numerical study of the natural convection heat transfer in rectangular enclosures filled with a nanofluid using the finite difference method with the stream function vorticity formulation. They investigated the effects of the Rayleigh number, the aspect ratio of the enclosure, and the volume fraction of the nanoparticles on the heat transfer inside the enclosures. Their results showed that the average heat transfer coefficient increased with increasing the volume fraction of the nanoparticles. Recently, an experimental study of natural convection heat transfer of nanofluid in vertical square enclosures was studied by Ho et al. [16]. They concluded that the average heat transfer rate depends on the thermophysical properties of the nanofluid and the heat transfer enhancement for nanofluid is more than that of for the pure water at high Rayleigh number. Abu – Hijleh [17] investigated numerically the effect of using permeable fins on the outer surface of a horizontal cylinder. He concluded that using permeable fins provides much higher heat transfer rates than solid fins. However, he assumed that the fin thickness is very small ( $d=0$ ) and it has a very high thermal conductivity (i.e.  $k_s=\infty$ ). These assumptions eliminate the need for simulating the region inside the permeable (porous) fins. In the current work, these assumptions are relaxed. Therefore, the relevant continuity, momentum and energy equations are solved in the porous media.

More recently, Kiwan [18] proposed a simple method using Darcy's model to solve the natural convection heat transfer from a single porous fin attached to a vertical surface. He found that the simple model equation can predict the heat transfer rates obtained based on complex models within  $\pm 10\%$  accuracy. Mokhtari Moghari et al. [19] studied two phase mixed convection  $\text{Al}_2\text{O}_3$  – water nanofluid flow in an annulus. They found that the Nusselt number increases by increasing volume fraction of nanoparticles at inner and outer cylinder, but it did not have any significant effect on the friction factor. Also, the value of the Nusselt number on the inner cylinder is more than that of on the outer cylinder. Thermal conductivity variation on natural convection flow of water – alumina nanofluid in an annulus is investigated by Parvin et al. [20] Two thermal conductivity models namely, the Chon et al. model and the Maxwell – Garnett model, are used to evaluate the heat transfer enhancement in the annulus. It is found that heat transfer rate enhancement is carried out by increasing volume fraction of nanoparticles and the Prandtl number at moderate and large Grashof number using both models but for Chon model, it had greatest value. The experimental work in this area is very limited. Kim et al. [21] investigated experimentally the impact of using porous fins on the heat transfer and flow characteristics in plate fin heat exchanger. However, their experiment was conducted under forced convection heat transfer conditions.

The main objectives of the present work is to study the effect concentration of nanoparticles, types of nanoparticles, without fins, solid fins and porous fins attaching at the inner cylinder on the heat transfer and flow in the annulus. As well as the effects of changing fin and annulus angles, Rayleigh number on the heat transfer are investigated and to compare the results with those obtained for without fins, solid (impermeable) fins and porous (permeable) fins by using nanofluids.

**Problem description and governing equation**

The physical model of the investigated problem consists of two concentric cylinders trapping nanofluid in the resulting annular cavity as illustrated schematically in Figs.(1) and (2). The inner cylinder and two fins are maintained at constant wall temperature (CWT), while the outer cylinder is diathermal (adiabatic). Two porous and solid fins of height of  $L_f$  and thickness of  $d$  are placed on the inner cylinder. The fin thickness  $d$  is kept constant in current analysis  $d = 2$  mm. the angle between the two fins is  $180^\circ$ . The annulus between the two cylinders is filled with water based nanofluid. Two types of nanoparticles (Cu and  $ZrO_2$ ) are investigated. It is assumed that the base fluid (distilled water) and nanoparticles are in thermal equilibrium and no slip occurs between them. The thermo – physical properties of the base fluid (distilled water) and the two types of nanoparticles forming the nanofluids are given in Table 1. The governing equations that describe the case are divided into two zones, the clear fluid zone and the porous zone. Therefore, two sets of equations are considered (continuity, momentum and energy equations). A set for clear domain (1) and another set for porous domain (2). The governing equations (continuity, momentum and the energy equations in the polar three – dimensional coordinate) for the case of single phase, laminar, steady flow and the porous medium is isotropic in cylindrical coordinates are as follows:

Continuity Equation in clear domain fluid (1):

$$\frac{\rho_{nf}}{r} (ru)_r + \frac{\rho_{nf}}{r} V_\theta + \rho_{nf} W_z = 0 \quad (1)$$

Momentum Equation in clear domain is:

r – Component

$$\rho_{nf} \left( VV_r + \frac{W}{r} V\theta - \frac{W^2}{r} \right) = -P_r + \mu_{nf} \left( V_{rr} + \frac{1}{r} V_r + \frac{1}{r^2} V_{\theta\theta} - \frac{V}{r^2} - \frac{2}{r^2} W_\theta \right) - \rho_{nf} g (\cos\theta \cos\alpha) \quad (2)$$

$\theta$  – Component

$$\rho_{nf} \left( VW_r + \frac{W}{r} W\theta - \frac{VW}{r} \right) = -\frac{1}{r} P_\theta + \mu_{nf} \left( W_{rr} + \frac{1}{r} W_r + \frac{1}{r^2} W_{\theta\theta} - \frac{W}{r^2} + \frac{2}{r^2} V_\theta \right) - \rho_{nf} g (\sin\theta \cos\alpha) \quad (3)$$

Z – Component

$$\rho_{nf} \left( VU_r + \frac{W}{r} U\theta \right) = -P_z + \mu_{nf} \left( U_{rr} + \frac{1}{r} U_r + \frac{1}{r^2} U_{\theta\theta} \right) - \rho_{nf} g (\sin\alpha) \quad (4)$$

Energy equation in clear domain is:

$$\rho_{nf} C_{p_{nf}} \left( Vt_r + \frac{W}{r} t_\theta + Wt_z \right) = k_{nf} \left[ -\frac{1}{r} \frac{\partial}{\partial r} (rt_r) + \frac{1}{r^2} t_{\theta\theta} + t_{zz} \right] \quad (5)$$

Continuity equation in the porous domain (2):

$$\frac{1}{r} \frac{\partial}{\partial r} (ru_r) + \frac{1}{r} \frac{\partial}{\partial \theta} (ut) + \frac{\partial \omega}{\partial z} = 0 \quad (6)$$

Momentum equations in the porous domain

According to the Darcy law done neglected non – Darcy effects which including the inertia force effect, boundary effect, channeling effect, thermal diffusion and assumed an inclined angle of the annulus ( $\alpha$ ) from horizontal axis. according to the assumptions mentioned the velocities components in cylindrical coordinate as follows:

$$u_r = \frac{-k}{\mu} \left( \frac{\partial P}{\partial r} - \rho g \cos\theta \cos\alpha \right) \quad (7)$$

$$ut = \frac{-k}{\mu} \left( \frac{\partial P}{\partial \theta} + \rho g \cos\theta \sin\alpha \right) \quad (8)$$

$$\omega = \frac{-k}{\mu} \left( \frac{\partial P}{\partial z} \pm \rho g \sin \theta \right) \tag{9}$$

Energy Equation in the porous domain

$$u_r \frac{\partial t}{\partial r} + \frac{u_t}{r} \frac{\partial t}{\partial \theta} + \omega \frac{\partial t}{\partial z} = \alpha_e \left[ \frac{1}{r} \frac{\partial}{\partial r} \left( r \frac{\partial t}{\partial r} \right) + \frac{1}{r^2} \frac{\partial^2 t}{\partial \theta^2} + \frac{\partial^2 t}{\partial z^2} \right] \tag{10}$$

The properties of nanofluid (fluid containing suspended nanoparticles) are defined as follows:  
 Effective thermal conductivity [22].

$$\frac{k_{nf}}{k_f} = \left[ \frac{k_s + (n-1)k_f - (n-1)(k_f - k_s)\Phi}{k_s + (n-1)k_f + (k_f - k_s)\Phi} \right] \tag{11}$$

Where n is a shape factor and equal to 3 for spherical nanoparticles.  
 Thermal diffusivity [23].

$$\alpha_{nf} = \frac{k_{nf}}{(1-\Phi)(\rho C_p)_f + \Phi(\rho C_p)_s} \tag{12}$$

Thermal expansion coefficient [24].

$$\beta_{nf} = \left[ \frac{1}{1 + \frac{(1-\Phi)\rho_f}{\Phi\rho_s}} \beta_s + \frac{1}{1 + \frac{\Phi}{(1-\Phi)\rho_f}} \beta_f \right] \tag{13}$$

Specific heat [24].

$$Cp_{nf} = \frac{(1-\Phi)(\rho C_p)_f + \Phi(\rho C_p)_s}{(1-\Phi)\rho_f + \Phi\rho_s} \tag{14}$$

Effective viscosity [23].

$$\mu_{nf} = [123\Phi^2 + 7.3\Phi + 1] \tag{15}$$

**Table .1.Thermo – physical properties**

Base fluid	Pr	ρ (Kg/m <sup>3</sup> )	Cp (J/kg K)	K (W/m K)	β X10 <sup>-5</sup> (K <sup>-1</sup> )	α X10 <sup>-5</sup> (m <sup>2</sup> /s)
Distilled water	6.2	997.1	4179	0.613	21	
Nanoparticles						
Copper (Cu)		8933	385	401	1.67	11.7
Zirconium oxide (ZrO <sub>2</sub> )		5890	278	22.7		12.4

**Boundary conditions**

A. With porous (permeable) fins case

The B.C of the model is derived based on the Darcy model. It is assumed that the boundaries slip with a symmetry about the vertical axis of the tube.

$$\frac{\partial T}{\partial R}(1, \theta, Z) = 0.5 \quad , \quad \frac{\partial T}{\partial \theta}(R, 0, Z) = 0 \quad , \quad \frac{\partial T}{\partial \theta}(R, \pi, Z) = 0$$

Inlet ( Z = 0),  $T(R, \theta, 0) = 0$

$$\frac{\partial \psi}{\partial R}(R, 0, Z) = 0 \quad \psi(R, \pi, Z) = 0$$

$$\frac{\partial \psi}{\partial R}(R, \pi, Z) = 0 \quad \psi(R, 0, Z) = 0$$

B. With solid (impermeable) fins case

$$\begin{aligned} U = V = W &= 0 & R=0, 1 \\ T &= 1 & R=0 \\ T &= 0 & R=1 \\ U = V = W &= 0 & \text{on fin's surfaces} \end{aligned}$$

$$U = V = \frac{\partial W}{\partial \theta} = 0 \text{ and } \frac{\partial T}{\partial \theta} = 0 \quad \text{on the left and right side of the solution domain}$$

$$k_r = \left. \frac{\partial T}{\partial R} \right|_{\text{fin}} = - \frac{k_{\text{nf}}}{k_f} \left. \frac{\partial T}{\partial R} \right|_{\text{nf}} \quad R = l_{\text{fin}}$$

Where,  $k_r$  is the ratio of fin conductivity to the conductivity of base fluid.

### Grid testing and code validation

Figs. (1) and (2) shows the geometry of the considered problem. Basically, the flow region associated with the polar coordinates  $(R, \theta)$  is divided into a grid network which contains the following dimensions  $(\Delta R \times \Delta \theta)$  for one division as shown in these figures. The number of divisions and nodal points in this case will be  $(m_t \times n_t)$  and  $[(m_t + 1) \times (n_t + 1)]$ , respectively, where  $m_t$  refers to the number of divisions in  $R$  direction which changes from  $(m = 1)$  to  $(m = m_t)$  and equal to  $(1/\Delta R)$ , while  $(n_t)$  refers to the number of divisions in  $\theta$  – direction which changes from  $(n = 1)$  to  $(n = n_t)$  and is equal to  $(\pi/\Delta \theta)$  for one half of the annulus gap because of flow symmetry about the vertical line of the annulus. The grid points are not distributed uniformly over the computational domain as shown in Figs.(3 – 5). They have greater density near surfaces of the inner and outer surfaces of the annulus and the surface of the fins. Fig.(6) shows mesh for flow region with porous fins and Fig.(7) demonstrates the influence of number of grid points for a test case of fluid confined within the present configuration at  $Ra=10^4$  and  $\Phi = 0$ , it is clear that, the grid system of  $(60 \times 80)$  is enough to obtain accurate results and guarantees.

Fig.(8) shows the variation of normalized local Nusselt number on the inner and outer cylinder surfaces. The results of Kuhen and Goldstien [25] and Sheikhzadeh et al., [26] for the same problem are also shown in this figure. In this comparison, the normalized local Nusselt number is defined as [28]:

$$k_{\text{eq}} = \frac{Nu_{i,o}}{\ln\left(\frac{D_o}{D_i}\right)} \quad (16)$$

The excellent agreement is observed between the present results and the results of Kuhen and Goldstien[1] and Sheikhzadeh et al.,[26]. In Fig (9) the variation of temperature versus radial direction for various angles are compared with the experimental results of Kuhen and Goldstien [25] and numerical result of Sheikhzadeh et al.,[26]. Good agreement between the present results and the previous results of Kuhen and Goldstien[25] and Sheikhzadeh et al.,[26].

### Numerical implementation

The governing equations in the cylindrical coordinates (equations 1 – 10 ) as well as boundary conditions were discretized by finite difference method. In this study the finite difference equations were derived by using central difference approximation for the partial derivatives except the convective terms for which upwind difference formula was employed. Derivative at the boundary were approximated by three point forward difference. The alternating direction implicit (ADI) method was employed for the solution of energy, while the momentum and continuity equations were combined as the pressure correction formula and solved by the simple algorithm. A time increment  $\Delta t = 10^{-5}$  has been used for  $Ra=10^3, 10^5$  and  $10^6$ . In order to evaluate how the presence of the nanofluids affect . the heat transfer rate around the perimeter of inner cylinder for various values of Rayleigh number, nanoparticles volume fraction, and inclination angles of the annulus it is necessary to observe the variation of the

Local Nusselt number on the perimeter of inner cylinder. To show the effect of the nanofluids on heat transfer rate, a variable called Nusselt number ratio (NuR) is introduced with its definition given as:

$$\text{NuR} = \frac{\text{Nuave|with nanofluid}}{\text{Nuave|pure fluid}} \quad (17)$$

If the value of NuR greater than 1 indicated that the heat transfer rate is enhanced on that fluid, whereas reduction of heat transfer is indicated when NUR is less than 1.

The local and average nusslet numbers on the surface of the fins is defined as:

$$\text{Nu}_{\text{fin}} = -\frac{2r_i k_{\text{eff}}}{1 k_f} \frac{\partial T}{R \partial \theta} \quad (18)$$

$$\text{Nu}_{\text{fin avg}} = \frac{1}{L_{\text{fin}}} \int_0^{l_{\text{fin}}} \text{Nu}_{\text{fin}} dR \quad (19)$$

Where ,  $k_{\text{eff}}$  is defined as:

$$k_{\text{eff}} = \frac{2k_{\text{fin}} k_{\text{nf}}}{k_{\text{fin}} + k_{\text{nf}}} \quad (20)$$

## Results and discussion

In his article, numerical calculations have been performed to porous fins, solid (impermeable) fins, without fins in the annulus. This article includes study the effect of using nanofluids through porous fins, solid fins and without fins on the heat transfer and flow. As well as the effect of changing Rayleigh number, volume fraction, fin angle, annulus angle and type of nanoparticles are considered. The inner cylinder is maintained at constant wall temperature and the outer cylinder is diathermal (adiabatic). The results are obtained for various Rayleigh numbers ( $Ra=10^3, 10^4, 10^5$ ), volume fractions of (1%, 2%, 3% , 5 %), fins inclination angles and annulus inclination angles ( $30^\circ, 60^\circ, 90^\circ$ ). Two types of nanoparticles are used which are Cu (30nm) and  $ZrO_2$  (50nm).

Fig. (11) depict secondary flow(on the left side) and isotherms (on the right side) inside the annulus. The existence of solid fin resists natural circulation in the annulus compared to finless annulus. However, the resistance of porous fins to the circulation is less than that of the solid fins. Consequently, the heat transfer from annulus with porous fins will be enhanced and greater than solid fins and without fins in the annulus. The secondary flow to the porous fins in annulus by using nanofluids (Cu (30nm) – DW ) and ( $ZrO_2$  (50nm) – DW ) are greater than distilled water at all Rayleigh number as a shown in these figures due to nanoparticle and convection strength is a very high. The vortex strength increases with Rayleigh number, and finally the vortex breaks up into two vortices at high Rayleigh number ( $Ra=10^5$ ). The secondary flow for two types of nanofluids at porous fins case is greater than solid fins and without fins in annulus due to the resistance of porous (permeable) fins to the circulation is less than of the solid (impermeable) fins.

Figs. (11) on the right side reveals isotherms. In general by increasing Rayleigh number, convection heat transfer increases and the plume region becomes more obvious. The isotherm concentration in annuli around the inner cylinder and across porous fins is more than other places between two cylinders. The gradient temperature becomes smaller and the boundary layer becomes thicker at  $Ra = 10^5$ . Minimum temperature of the nanofluid is smaller than distilled water due to nanoparticle and two types of nanofluids.

The isotherms in the annulus region indicate that the heat transfer is concentrated around the bottom of the inner cylinder and at upper part of outer cylinder.

Figs.(12) shows when adding Cu (30nm) and  $ZrO_2$  (50nm) nanoparticles in distilled water increases the effective thermal conductivity of the nanofluids and therefore the molecular heat diffusion is augmented. The vortex strength is similar approximately between nanofluids and distilled water. It can be noticed small second eddy formed below porous fins and solid fins as well as without fins in annulus which pushing the main eddy to upward and making unsymmetrical. The secondary flow does not significantly change despite of higher heat flux needs to keep the Rayleigh number constant for higher particles concentration.

Figs. (13) shows the effects of angles inclination to fins and annulus on the secondary flow and isotherms. The vortex strength through the porous fins intensifies as the inclination angle decreases where it reaches the maximum at horizontal position of the fin. Consequently this case is similar to the case without fins in annulus except angle of annulus ( $\alpha = 90^\circ$ ) the main and secondary flow are in the same direction, so the vortex strength diminishes by using nanofluids. Thus, there is no tangential and radial velocities, and the value of secondary flow in terms of these two velocities is equal to zero. In case of the solid (impermeable) fin, the heat transfer increases as the inclination angle increases where it reaches maximum at vertical position when using nanofluids.

Fig.(13) reveal that the nanofluid circulates in a vortex– shaped pattern and the circulation centers move up as Rayleigh number increases. The nanofluid moves up along the inner cylinder and falls down along the outer cylinder. The velocity of nanofluid is very low near the circulation centers. As the Rayleigh number increases, the boundary layer along the inner and outer cylindrical surfaces can be observed and high velocity and temperature gradients exist near the inner and outer surfaces. The shape of the secondary flow indicates that the flow pattern intensifies as well as moves upward as the temperature difference increases. The results also shows that as the fin inclination angle increases the fins push the circulation up which squeezes the boundary layer along upper half of the outer cylinder. This effect is similar to effect of increasing Rayleigh number in case without fins in annulus, i.e., an increase in heat transfer. The heat transfer increases as inclination angle increases for solid (impermeable) fins. However for porous(permeable) fins, the opposite is true i.e., increasing inclination angle decreases heat transfer at using nanofluids .

The flow through the porous fins, as shown in the figures (11 – 13 ), has the following effects on the nature of the flow in the gap between the two cylinders these effects including on it destroys the boundary layer along the upper part of the fins , it decreases boundary layer thickness along lower surfaces of the fins and squeezes boundary layer along outer cylinder. Consequently, the presence of porous (permeable) fins and nanoparticles are expected to increase the heat transfer through the annulus.

Fig.(14) shows the variations of local Nusselt number on the fins' surfaces and inner cylinder surface of the two types of nanofluids (Cu(30nm),ZrO<sub>2</sub> (50nm) – DW) for three cases of annulus with porous fins , with solid (impermeable) fins, without fins. This figure indicated that the local Nusselt number of the nanofluids are greater than distilled water due to nanoparticles and high Rayleigh number. The local Nusselt number of the nanofluid (Cu(30nm) – DW) is greater than nanofluid (ZrO<sub>2</sub> (50nm) – DW) due to high thermal conductivity for copper in comparison with zirconium oxide

As well as this figure depicts that that comparing to without fins case, the use of solid and porous fins enhances the heat transfer only in the upper half of the around inner cylinder by using nanofluids (Cu(30nm) – DW) and (ZrO<sub>2</sub>(50nm) – DW).

The enhancement in heat transfer of nanofluids for annulus with porous fins, solid (impermeable) fins and annulus without fins at (5 %) volume concentration of (Cu) nanoparticles increases (82.25 %, 70.15 %,50.33 % ) while of (ZrO<sub>2</sub>) (69.35 %, 52.44 %,37.42 % ) respectively compared with the base fluid (distilled water).

Fig.(15) reveal the axial profile of the peripheral Nusselt number with different configuration, volume fraction ( $\Phi = 1\%, 3\%, 5\%$ ), Rayleigh number ( $Ra=10^3, 10^4, 10^5$ ), Length of fins ( $L=0.2$ ). From this figure can be clearly seen increasing the Rayleigh number augments the buoyancy force and enhances Nusselt number at the fully developed region. The enhancement heat transfer for the nanofluid (Cu (30 nm) – DW) is higher than nanofluid (ZrO<sub>2</sub>(50 nm) – DW) due to small nanoparticles size of copper, this makes the random motion larger and the convection effect become more pronounced. The two types of nanofluids, with 30 nm, and 50 nm nanoparticles showed higher heat transfer rate than the base fluid. The metallic nanoparticles give higher heat transfer enhancement than nonmetallic nanoparticles (oxides) due to the higher thermal conductivity of the metallic nanoparticles.

Fig. (16) shows the average skin friction coefficient for nanofluids (Cu(30nm) – DW) and (ZrO<sub>2</sub>(50nm) – DW). Despite augmenting the Nusselt number by increasing the nanoparticles concentration, the skin friction does not change. As it was seen in the previous figures and the secondary flow are not significantly affected by the nanoparticles concentration. Also at high Rayleigh numbers increasing the nanoparticles volume fractions does not have significant effect on skin friction coefficient. In general, increasing the annulus inclinations for three cases (porous fins, solid (impermeable) fins, without fins )augments the flow acceleration near wall and consequently higher skin friction occurs.

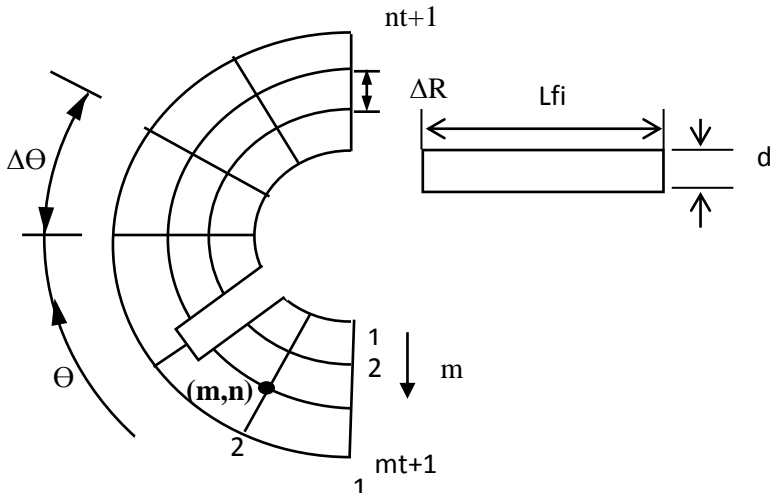


Fig (1) Physical representation for problem by polar coordinate with solid (impermeable) fin

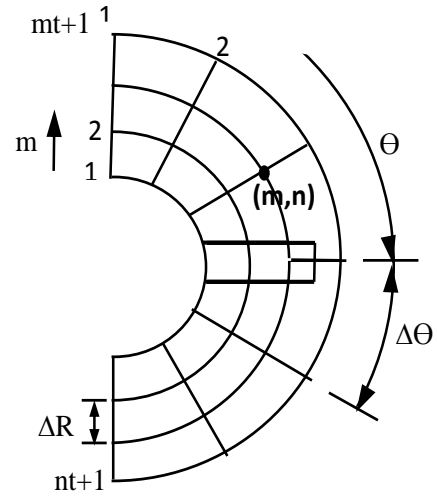


Fig (2) Physical representation for problem by polar coordinate with porous fin

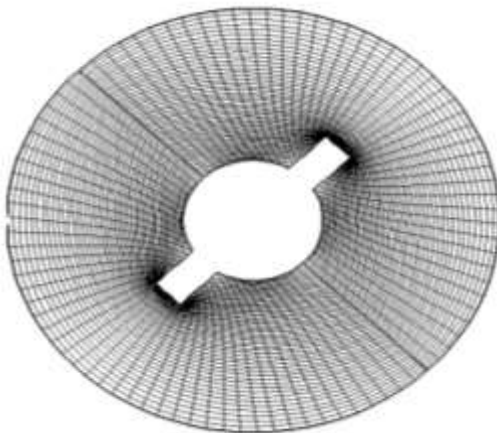


Fig (3) Mesh network for flow region representation with solid (impermeable) fin

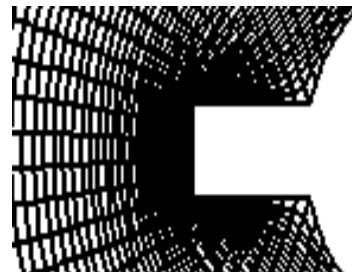


Fig (4) Grid near fin and inner surface

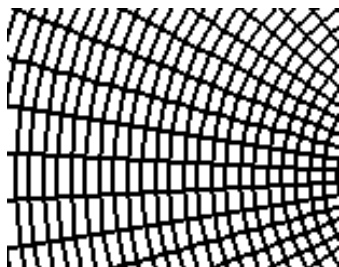


Fig (5) Grid near outer surface

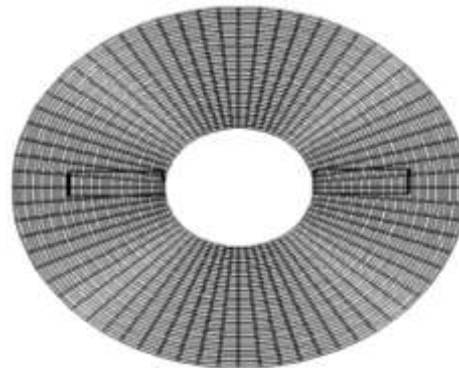


Fig (6) Mesh network for flow region representation with porous fins



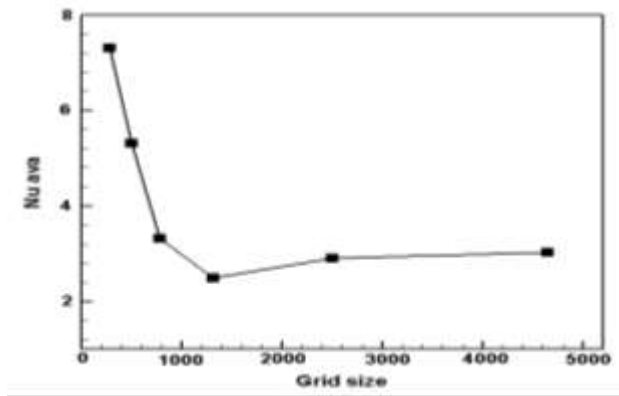


Fig.(7) Grid Size Study for  $Ra=10^4$ ,  $\Phi = 0$

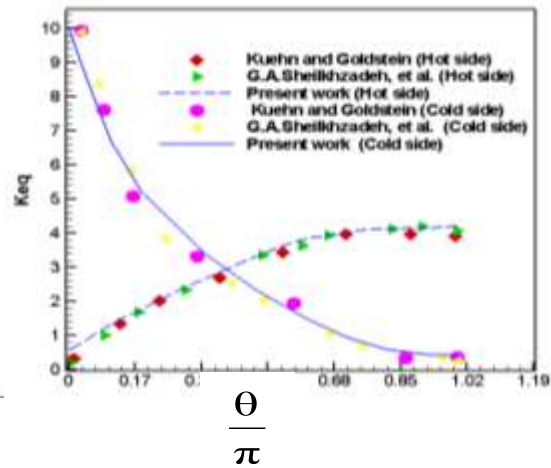


Fig.(8) Variations normalize of local Nusselt number on the inner and outer cylinder surfaces: comparison between the present work with the results [25,26]

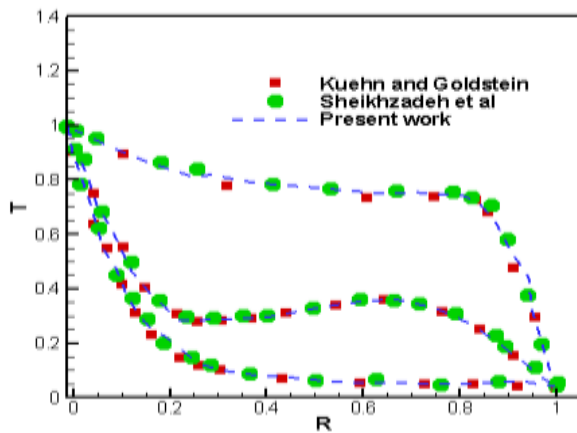


Fig.(9) Variation of temperature versus radial Direction: comparison between the Present work and the results [25,26]

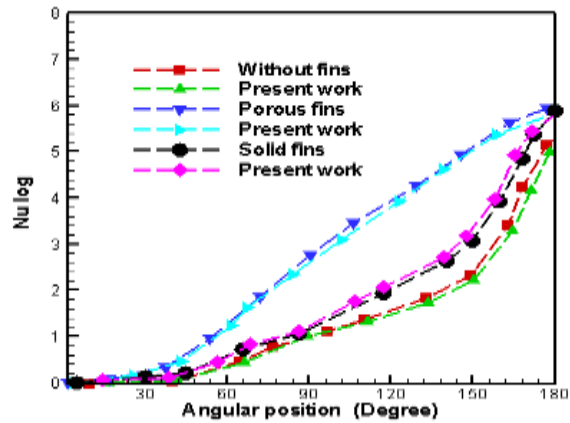


Fig.(10) Distribution of heat transfer at the inner cylinder at  $Da= 2.5 \times 10^{-3}$ ,  $Kr= 4 \times 10^3$ ,  $Ra = 10^4$  comparison between the Present work and the results [27]

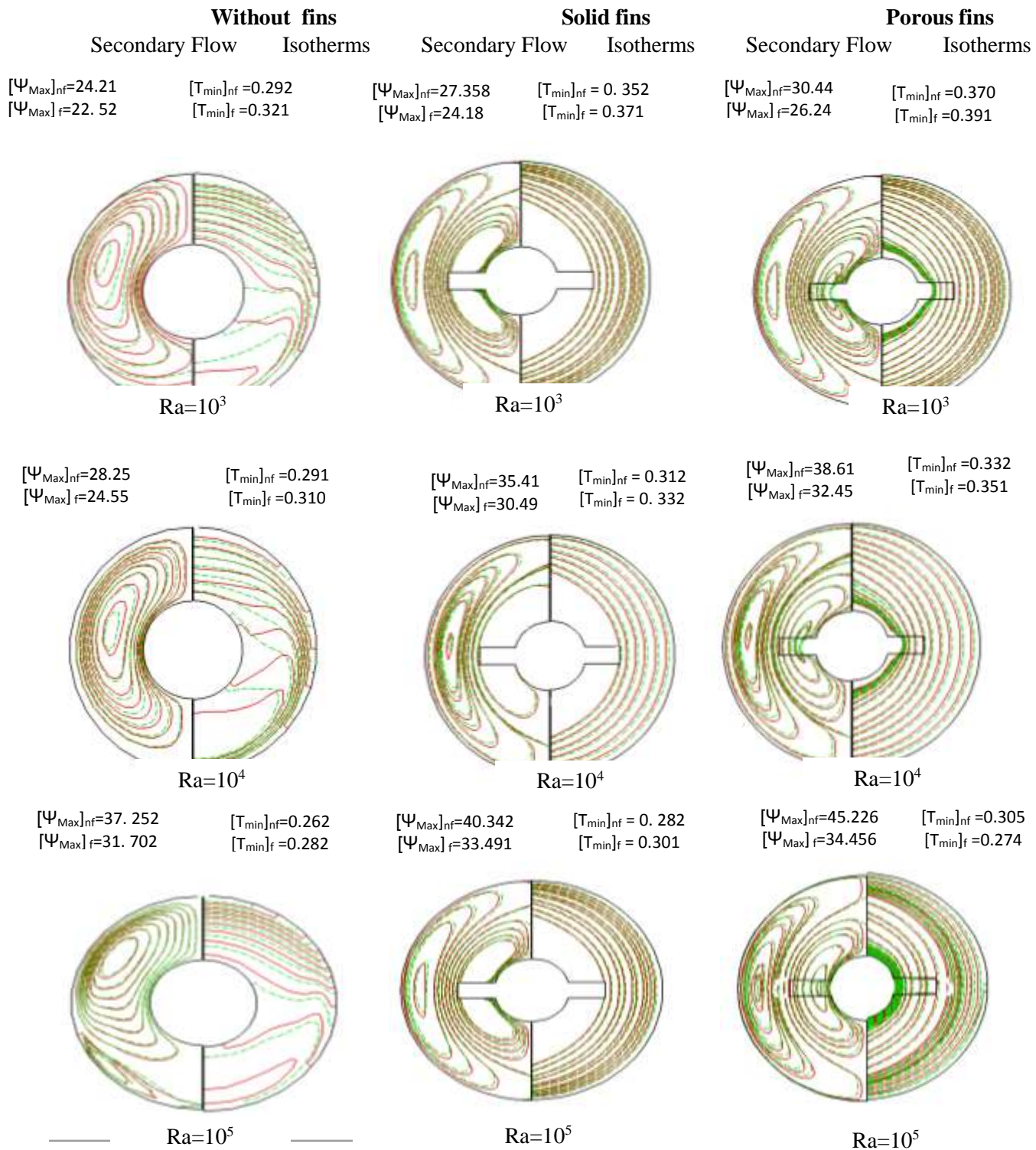


Fig.(11) : Secondary flow (on the left) and Isotherms (on the right) for Cu – distilled water nanofluids (—) and distilled water (----) with different Ra ,  $\Phi = 3\%$ ,  $\alpha_{fin} = 0^0$  and,  $L_{fin} = 0.2$

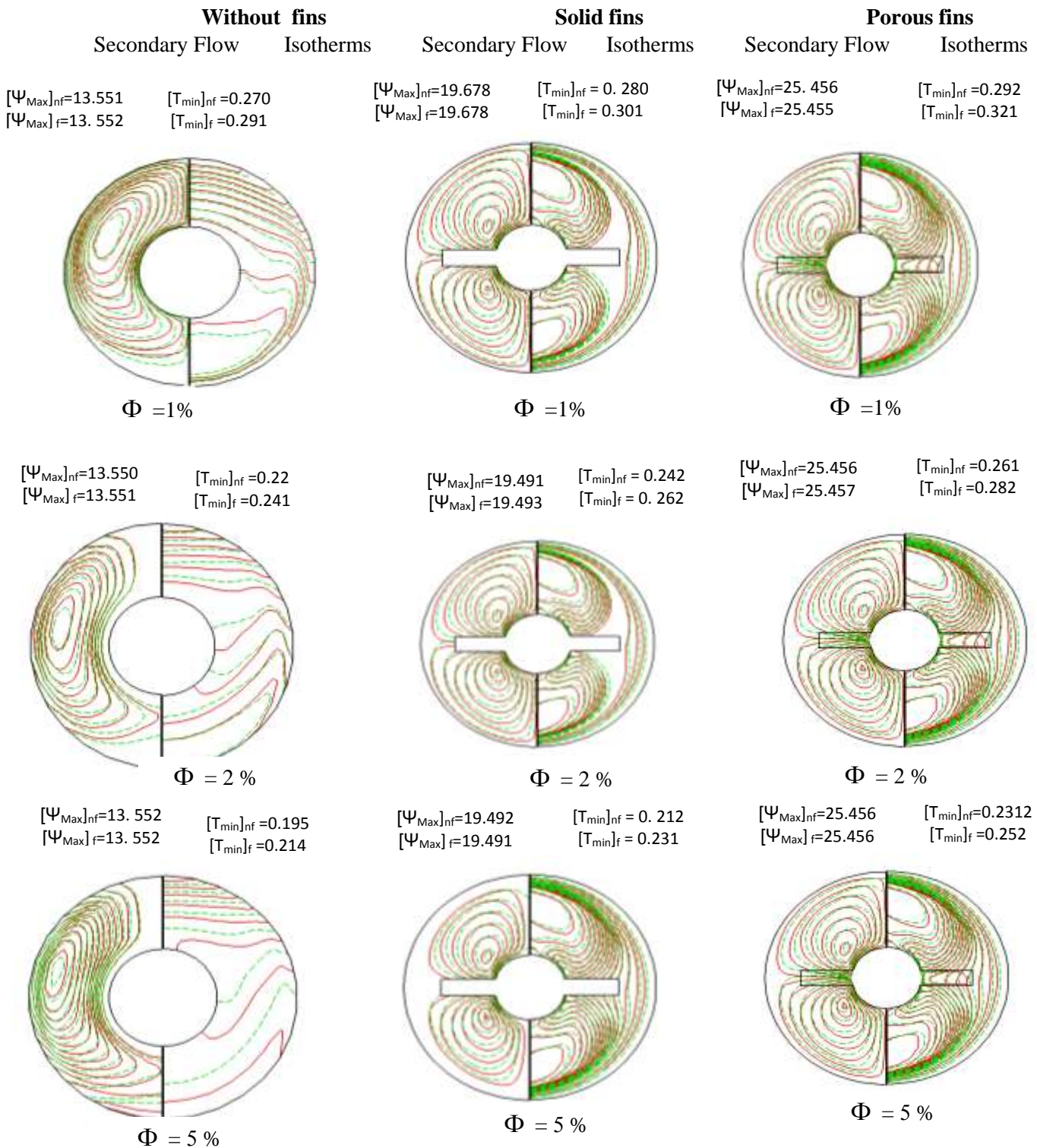
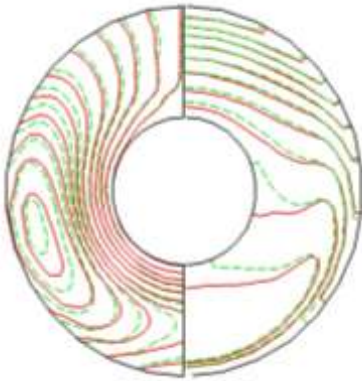


Fig.(12) : Secondary flow (on the left) and Isotherms (on the right) for Cu – distilled water nanofluids (—) and distilled water (----) with different  $\Phi$ ,  $Ra=10^5$ ,  $\alpha_{fin}=0^0$  and  $L_{fin}=0$ .

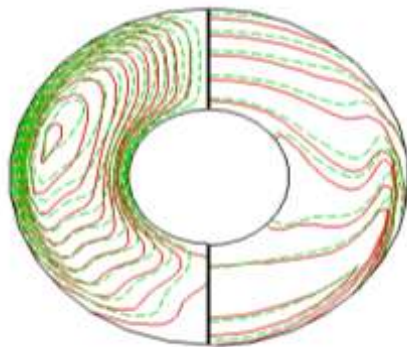
**Without fins**  
 Secondary Flow Isotherms

$[\Psi_{Max}]_{nf}=10.56$        $[T_{min}]_{nf}=0.310$   
 $[\Psi_{Max}]_f=8.213$        $[T_{min}]_f=0.342$



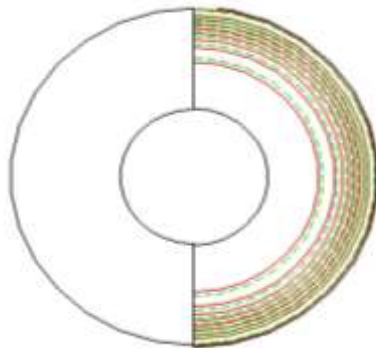
$\alpha_{anu}=30^{\circ}$

$[\Psi_{Max}]_{nf}=7.214$        $[T_{min}]_{nf}=0.270$   
 $[\Psi_{Max}]_f=5.23$        $[T_{min}]_f=0.293$



$\alpha_{anu}=60^{\circ}$

$[\Psi_{Max}]_{nf}=0.0$        $[T_{min}]_{nf}=0.195$   
 $[\Psi_{Max}]_f=0.0$        $[T_{min}]_f=0.264$



$\alpha_{anu}=90^{\circ}$

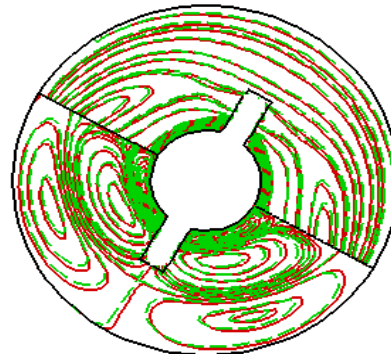
**Solid fins**  
 Secondary Flow Isotherms

$[\Psi_{Max}]_{nf}=8.492$        $[T_{min}]_{nf}=0.264$   
 $[\Psi_{Max}]_f=6.410$        $[T_{min}]_f=0.281$



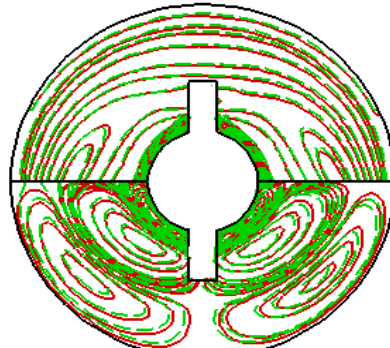
$\alpha_{fin}=30^{\circ}$

$[\Psi_{Max}]_{nf}=10.491$        $[T_{min}]_{nf}=0.392$   
 $[\Psi_{Max}]_f=8.321$        $[T_{min}]_f=0.413$



$\alpha_{fin}=60^{\circ}$

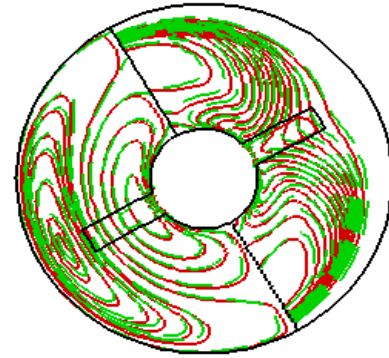
$[\Psi_{Max}]_{nf}=12.142$        $[T_{min}]_{nf}=0.331$   
 $[\Psi_{Max}]_f=11.122$        $[T_{min}]_f=0.359$



$\alpha_{fin}=90^{\circ}$

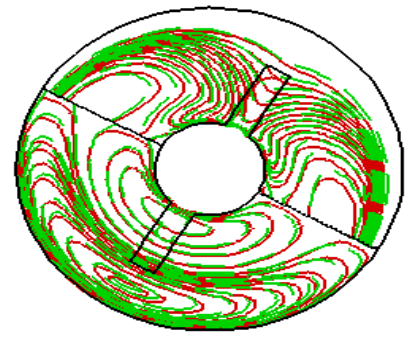
**Porous fins**  
 Secondary Flow Isotherms

$[\Psi_{Max}]_{nf}=15.420$        $[T_{min}]_{nf}=0.341$   
 $[\Psi_{Max}]_f=15.78$        $[T_{min}]_f=0.362$



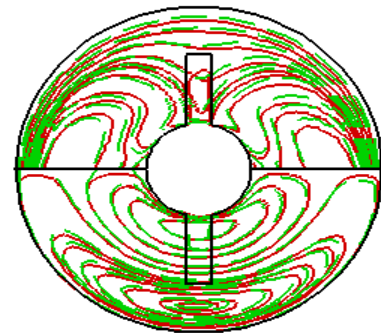
$\alpha_{fin}=30^{\circ}$

$[\Psi_{Max}]_{nf}=12.251$        $[T_{min}]_{nf}=0.312$   
 $[\Psi_{Max}]_f=11.421$        $[T_{min}]_f=0.332$



$\alpha_{fin}=60^{\circ}$

$[\Psi_{Max}]_{nf}=10.52$        $[T_{min}]_{nf}=0.27$   
 $[\Psi_{Max}]_f=9.55$        $[T_{min}]_f=0.2983$



$\alpha_{fin}=90^{\circ}$

Fig. (13) : Secondary flow (on the left) and Isotherms (on the right) for Cu – distilled water nanofluids (—) and distilled water (---) with different angles to fins and annulus,  $Ra=10^5$ ,  $\Phi = 3\%$  and  $L_{fin}=0.2$

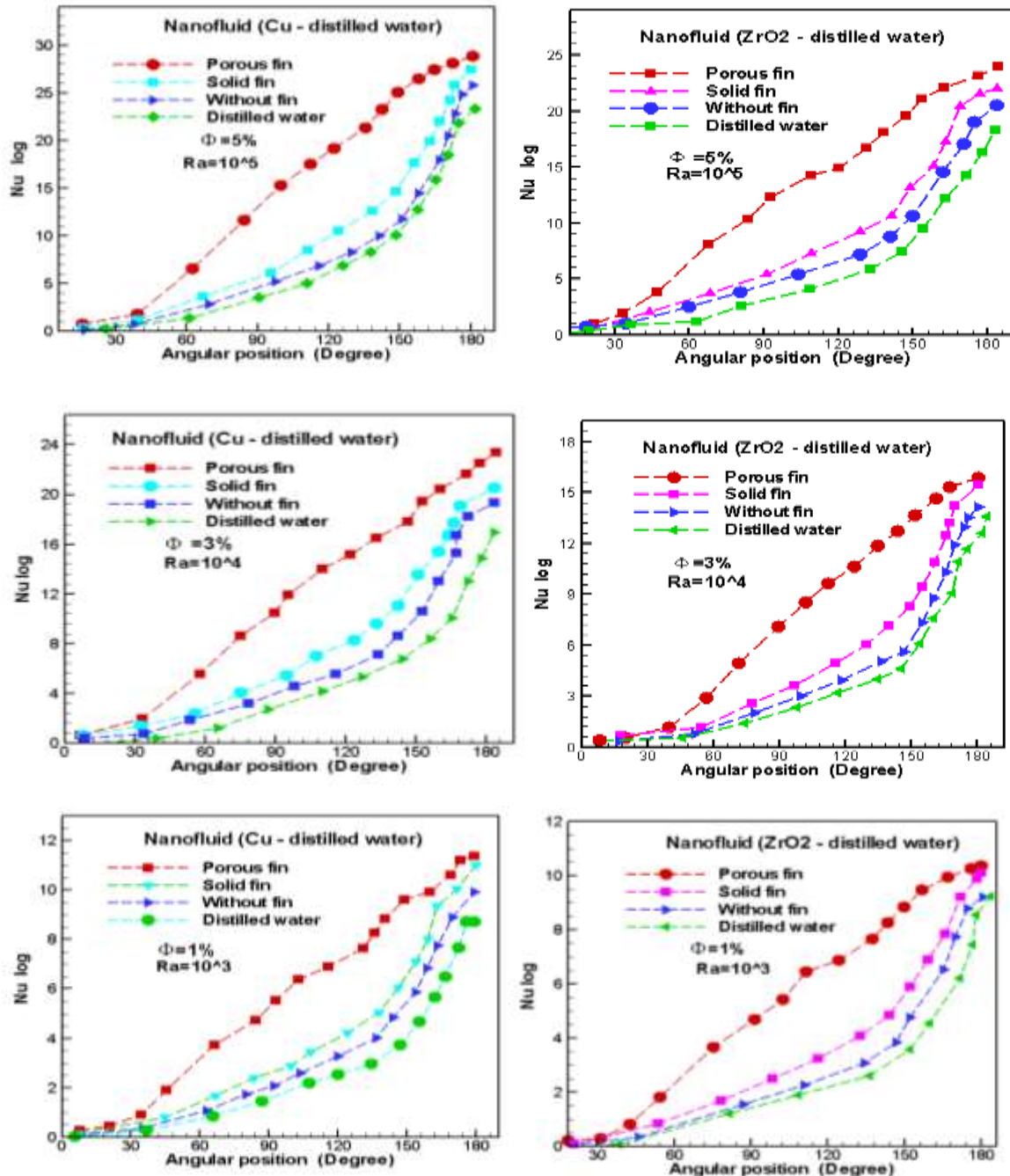


Fig. (14): Variation of local Nusselt number around the inner cylinder and fins surfaces for Cu and ZrO<sub>2</sub> – distilled water nanofluids with different  $\Phi$ , Rayleigh number and  $L_{fin}=0.2$

Cu – distilled water

ZrO<sub>2</sub> – distilled water

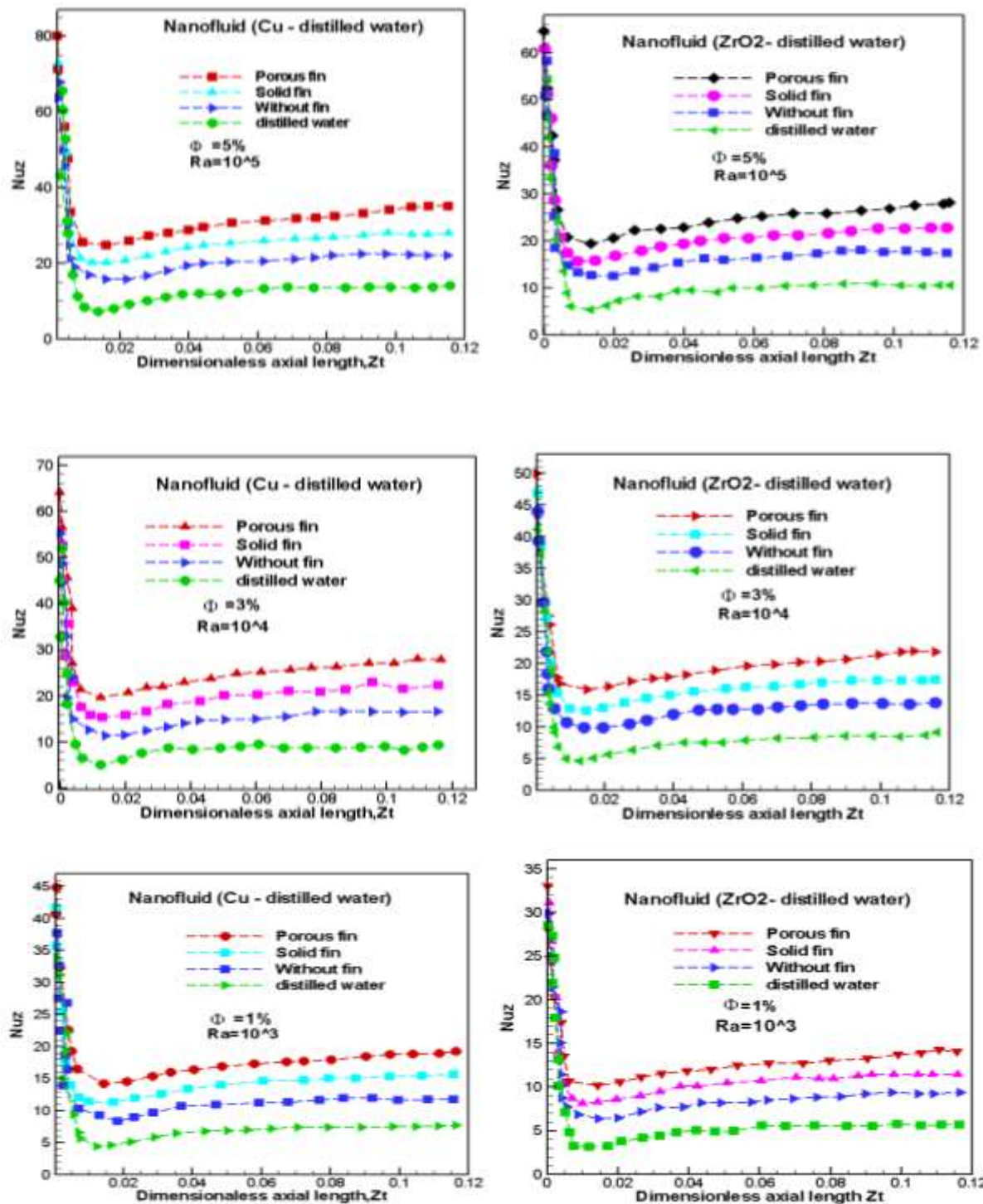


Fig. (15): Axial profile of the peripheral average Nusselt number to Cu, and ZrO<sub>2</sub> – distilled water nanofluids with different Rayleigh number, volume fraction and  $L_{fin} = 0.2$

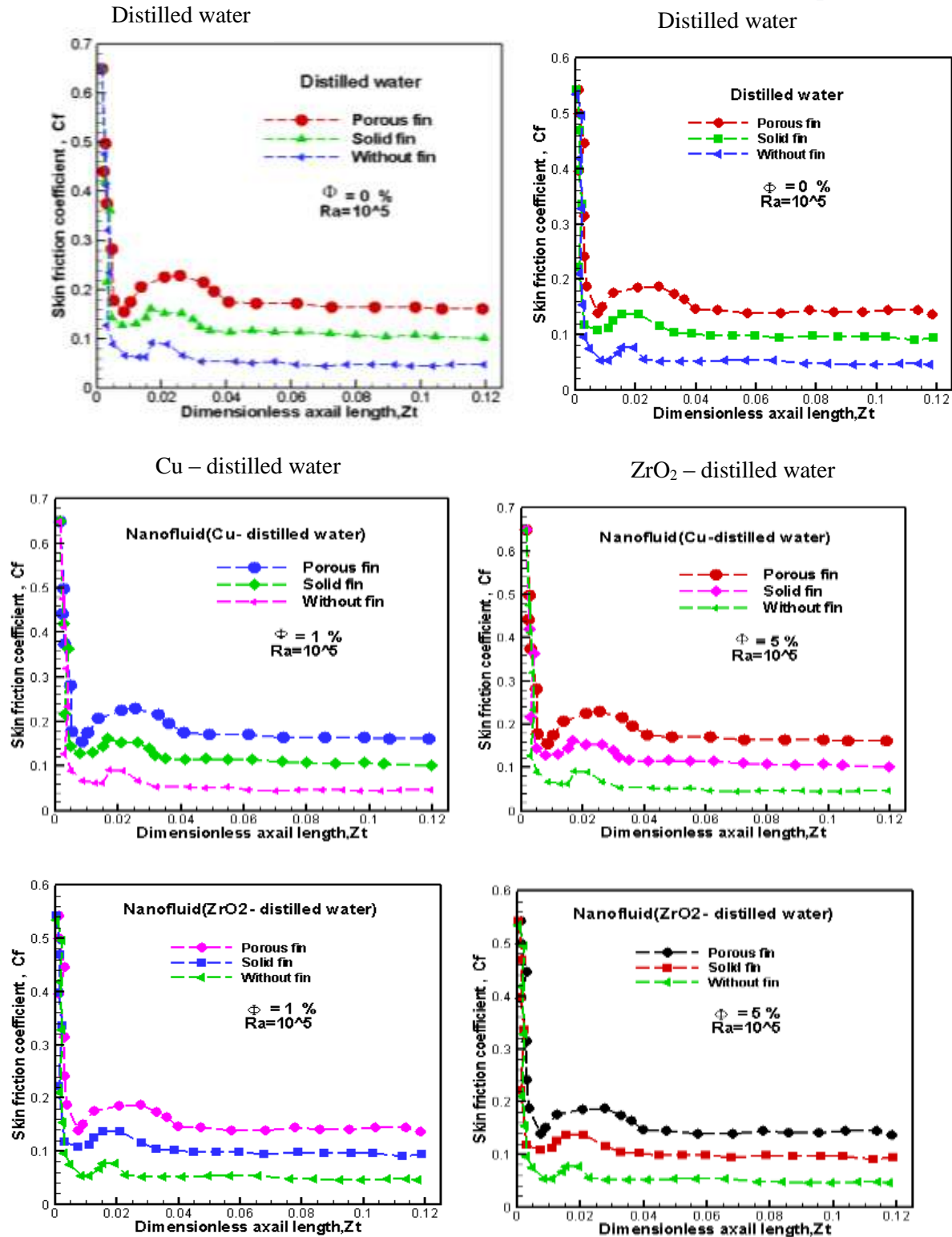


Fig. (16) : Axial profile of the peripheral average skin friction coefficient to nanofluid (Cu, ZrO<sub>2</sub> – distilled water) with different  $\Phi, Ra=10^5$  and  $L_{fin} = 0.2$

## Conclusion

The main conclusions of the present study are:

1. The highest heat transfer was obtained to Cu (30nm) and the porous fins due to domination of conduction and small nanoparticles. Therefore the choice of nanoparticles is very important in the convective heat transfer application.
2. As the solid volume fraction increases, the heat transfer is enhanced for all values of the Rayleigh number. This enhancement is more significant at high Rayleigh number.
3. The enhancement in heat transfer of nanofluids for annulus with porous fins, solid (impermeable) fins and annulus without fins at (5%) volume concentration of (Cu) nanoparticles increases (82.25 %, 70.15 %, 50.33 % ), while of (ZrO<sub>2</sub>) (69.35%, 52.44 %, 37.42 % ) respectively compared with the base fluid (distilled water).
4. The increase of the average Nusslet number is attributed to the increase of the thermal conductivity of nanofluid with increasing the volume fraction of the nanoparticles. However, the viscosity of nanofluid also increases with increasing the volume fraction of nanoparticles.
5. Skin friction coefficient does not change in porous (permeable) fins, solid (impermeable) fins and without fins in annulus.
6. The metallic nanoparticles give higher heat transfer enhancement than nonmetallic particles (oxides) due to the high thermal conductivity of metallic nanoparticles.

## Reference

1. Kuhen TH, Goldstein RJ An experimental and theoretical study of natural convection in the annulus between horizontal concentric cylinders. *Fluid Mech J* 74, 695–719, (1976).
2. Kuhen TH, Goldstein RJ An experimental study of natural convection heat transfer in concentric and eccentric horizontal cylindrical annuli. *ASME J Heat Transf* 100, 635–640, (1978).
3. Kumar R Study of natural convection in horizontal annuli. *Int J Heat Mass Transf* 31, 1137–1148, (1988).
4. Ho CJ, Li YH, Chen TC A numerical study of natural convection in concentric and eccentric horizontal cylindrical annuli with mixed boundary conditions. *Int J Heat Fluid Flow* 10, 40–47, (1989).
5. Yeh CL Numerical investigation of three – dimensional natural convection inside horizontal concentric annulus with specified wall temperature or heat flux convection in a horizontal annulus driven by inner heat generating solid cylinder. *Int J Heat Mass Transf* 45, 775–784, (2002).
6. Chai JC, Patankar SV Laminar natural convection in internally finned horizontal annulus. *Numer Heat Transf* 24, 67–87, (1993).
7. Rahnema M, Farhadi M Effect of radial fins on two dimensional turbulent natural convection in a horizontal annulus. *Int J Therm Sci* 43, 255–264, (2004).
8. Maxwell JC Electricity and magnetism. Clarendon Press, Oxford, UK, (1873)
9. Choi SUS Enhancing thermal conductivity of fluid with nanoparticles, developments and applications of non – Newtonian flow. *ASME FED* 231, 99–105, (1995).
10. Behzadmehr A, Saffar – Avval M, Galanis N Prediction of turbulent forced convection of a nanofluid in a tube with uniform heat flux using a two phase approach. *Int J Heat Fluid Flow* 28, 211–219, (2007).
11. Bianco V, Chiacchio F, Manca O, Nardini S Numerical investigation of nanofluids forced convection in circular tubes. *J Appl Therm Eng* 29, 3632–3642, (2009).
12. Santra AK, Sen S, Chakraborty N Study of heat transfer due to laminar flow of copper–water nanofluid through two isothermally heated parallel plates. *Int J Therm Sci* 48, 391–400, (2009).
13. Putra N, Roetzel W, Das SK Natural convection of nanofluids. *Heat Mass Transf* 39, (8–9):775–784, (2003).
14. Wen D, Ding Y Formulation of nanofluids for natural convective heat transfer applications. *Int J Heat Fluid Flow* 26(6), (2005):855–864
15. Jou RY, Tzeng SC Numerical research of nature convective heat transfer enhancement filled with nanofluids in rectangular enclosures. *Int Commun Heat Mass Transf* 33, 727–736, (2006).
16. Ho CJ, Liu WK, Chang YS, Lin CC Natural convection heat transfer of alumina-water nanofluid in vertical square enclosures: an experimental study. *Int J Therm Sci* 49(8), 1345– 1353, (2010).



17. Abu – Hijleh , B. A. K., “Enhanced forced convection heat transfer from a cylinder using permeable fins”, ASME J. Heat Transfer 125, 804-811, 2003.
18. Kiwan, S. M., “Thermal analysis of natural convection porous fins”, Accepted for publications in the Transport in Porous Media, 2006.
19. Mokhtari Moghari R, Akbarinia A, Shariat M, Talebi F, Laur R Two phase mixed convection  $Al_2O_3$ -water nanofluid flow in an annulus. Int J Multiph Flow 37(6), (2011):585–595
20. Parvin S, Nasrin R, Alim MA, Hossain NF, Chamkha AJ Thermal conductivity variation on natural convection flow of water–alumina nanofluid in an annulus. Int J Heat Mass Transf 55(19 – 20), 5268–5274, (2012).
21. Kim, S. Y., Paek, J. W. and Kang, B. H., “Flow and heat transfer correlations for porous fin in a plate-fin heat exchanger”, ASME J. Heat Transfer 122, 572 – 578 . 2000.
22. W. Daungthongsuk, S. Wongwises, A critical review of convective heat transfer nanofluids, Renewable and Sustainable Energy Reviews 11, ,797–817,(2007).
23. Barozzi, Sabbagh ,G.S., Zan chini, et al, "Experimental investigation of combined forced and free convection in Horizontal and inclined tubes". Meccanica 20, 18–27,(1985).
24. K. Khanafer, K. Vafai, M. Lightstone, Buoyancy – driven heat transfer enhancement in a two – dimensional enclosure utilizing nanofluids, International Journal of Heat and Mass Transfer 46, ,3639 – 3653,(2003).
25. Kuhen TH, Goldstein RJ An experimental and theoretical study of natural convection in the annulus between horizontal concentric cylinders. Fluid Mech J 74, 695–719, (1976).
26. G. A. Sheikhzadeh • M. Arbaban • M. A. Mehrabian Laminar natural convection of Cu – water nanofluid in concentric annuli with radial fins attached to the inner cylinder 012 – 1084 – 9 , October (2012).
27. S.Kiwan, O. Zeitoun, "Natural convection in a horizontal cylindrical annulus using porous fins", International Journal of Numerical Methods for Heat & Fluid Flow, Vol. 18 Iss: 5, pp.618 – 634, (2008).
28. Kenjeres S, Hanjalic K) Prediction of turbulent thermal convection in concentric and eccentric horizontal annuli. Int J Heat Fluid Flow 16, 429–439, (1995):.
29. D. H. Anderson, J. C. Tannehill, and R. H. Plecher“ Computational Fluid Mechanics and Heat Transfer” Hemisphere. Washington, DC (1984).

### Nomenclature

$r_i$	The annulus inner radius	m
$r_0$	The annulus outer radius	m
$Cp_{nf}$	Specific heat of nanofluid at constant pressure	kJ/kg.k
$g$	Gravity acceleration	$m/s^2$
$G$	Dimensionless gravity acceleration	–
$d$	The fin thickness	m
$L_{fin}$	Fin length	m
$R, \theta, Z$	Dimensionless cylindrical coordinates	–
$Nu$	Nusselt number	–
$S$	Relaxation factor	–
$T$	Temperature	$^{\circ}C$
$u$	Radial velocity component ( $r$ )	m/s
$v$	Tangential velocity component ( $\theta$ )	m/s
$w$	Axial velocity component ( $z$ )	m/s
$k_{nf}$	Thermal conductivity of the nanofluid	W/m.k
$P$	Dimensionless pressures	–
$d_p$	Particle diameter	nm
CWT	Constant wall temperature	–
ADI	Alternating direction implicit	–
DW	Distilled water	–
<b>Creak Symbols</b>		
$\alpha_{fin}$	Angle of inclination of fin	degree

$\alpha_{nf}$	Thermal diffusivity of the nanofluid	$m^2/s$
$\beta_{nf}$	Thermal Expansion Coefficient of the nanofluid	1/k
$\mu_{nf}$	Dynamic viscosity of the nanofluid	kg/m.s
$\nu_{nf}$	Kinematic viscosity of the nanofluid	$m^2/s$
$\rho_{nf}$	Density of the nanofluid	$kg/m^3$
$\Psi$	Stream function	$m^2/s$
$\Phi$	Volume fraction	Vol%
<b>Subscripts</b>		
mt	Number of radial points in the numerical mesh network	
nt	Number of tangential points in the numerical mesh network	
w	Wall	